SUPPLEMENTAL MATERIAL

Figure S1. pSTAT3-MerTK-galectin-3 axis regulates osteopontin expression in vitro.

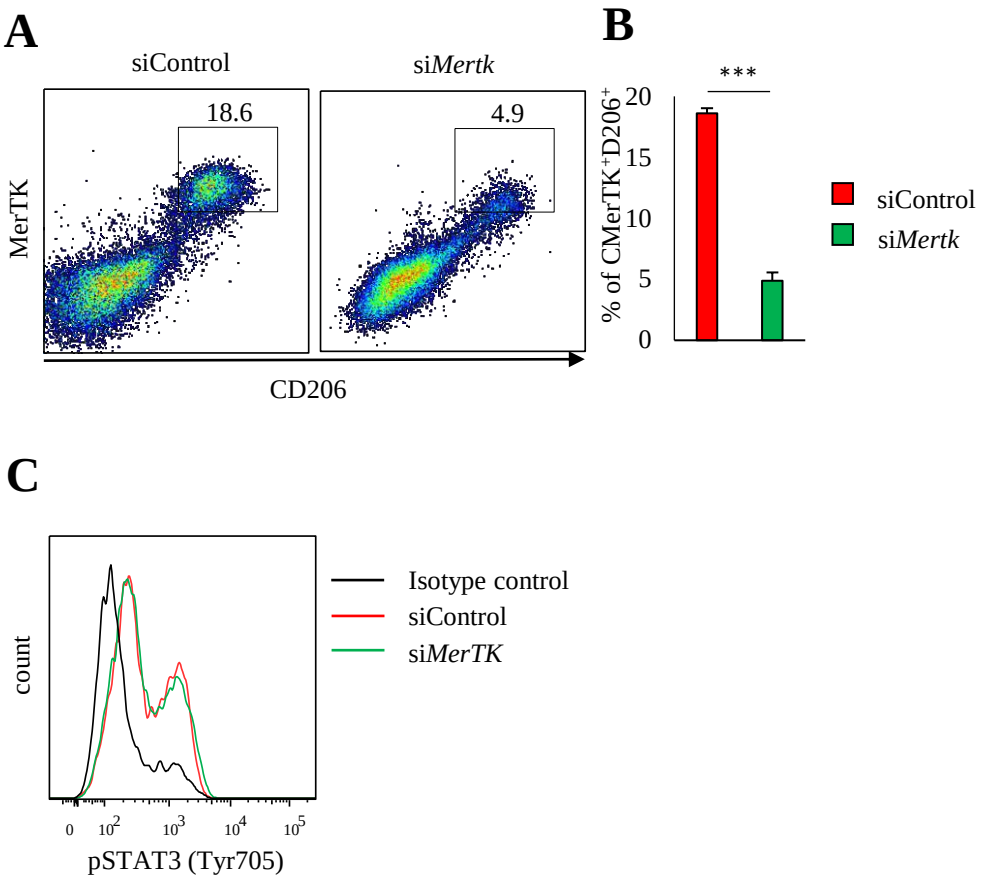

A CD11b$^+$Ly6G$^-$ cells (2 × 10^5) were sorted from bone marrow of 8- to 10-week-old WT mice and cultured for 3 days with rIL-10 + DMSO or rIL-10 + STAT3 inhibitor. Representative flow cytometric analysis of MerTK$^+$ on CD206$^+$ in CD11b$^+$ Ly6G$^-$ cells (**A**) and bar graphs enumerate MerTK$^+$ on CD206$^+$ in CD11b$^+$ Ly6G$^-$ cells (n = 5 per group) (**B**). Representative histogram of pSTAT3 (Tyr705) on CD11b$^+$ Ly6G$^-$ cells (**C**). Flow cytometric analysis was performed in at least three independent experiments. *P < 0.05, ***P < 0.001; n.s.: not significant. Data are mean ± SEM.

Figure S2. Apoptotic cells did not induce the transcriptional activity of Spp1.

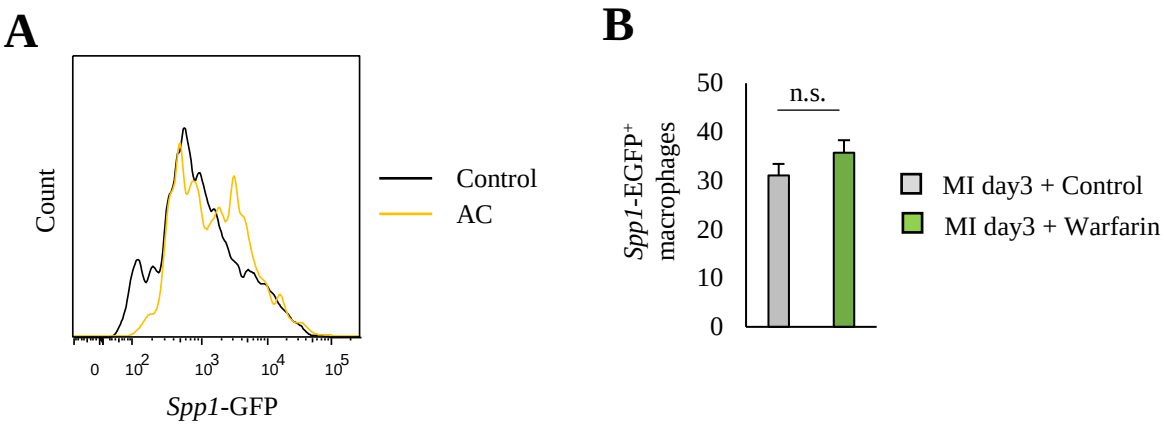

A Apoptotic cardiomyocytes treated with hydrogen peroxide and $CD11b^{+}Ly6G^{-}$ cells were co-cultured for 72 hours. Representative histogram *Spp1*-GFP in $CD11b^{+}Ly6G^{-}$ cells.
B DMSO or warfarin was administered via intravenous injection from 1 day before MI to post-MI day 3 into EGFP-*Spp1*-KI reporter mice. Bar graph shows the percentage of *Spp1*-GFP^{+} cells in cardiac macrophages (*n* = 4 mice per group)

Figure S3. pSTAT3-MerTK-galectin-3 axis regulates osteopontin expression in vivo.

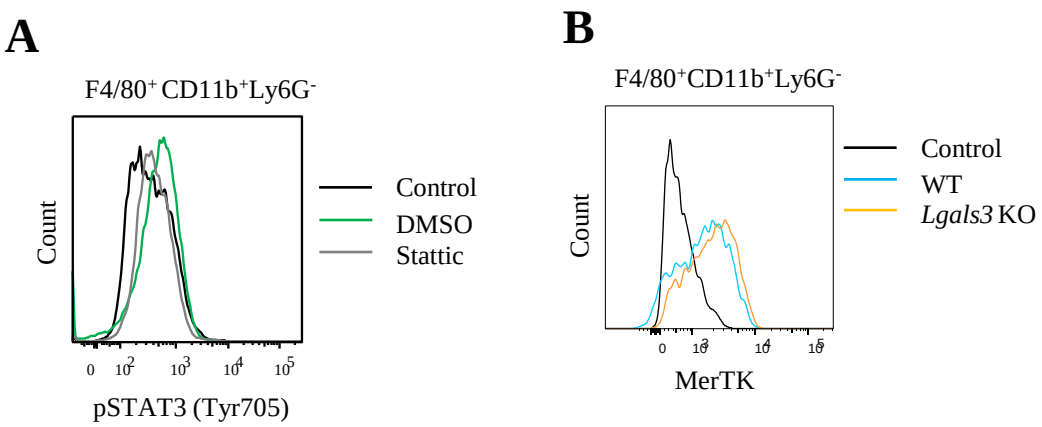

A DMSO or Stattic (STAT3 inhibitor) was administered via intraperitoneal injection from 1 day before MI to post-MI day 3 into WT mice. Representative histogram of pSTAT3 (Y705) on cardiac F4/80$^+$ CD11b$^+$Ly6G$^-$ cells of DMSO or Stattic-treated mice. **B** Representative histogram of MerTK on cardiac F4/80$^+$CD11b$^+$Ly6G$^-$ cells of post-MI hearts on day 3 of WT and *Lgals3*-KO mice. Flow cytometric analysis was performed in at least three independent experiments.

Figure S4. M-CSF is required for IL-10 to induce the differentiation of osteopontin-producing cells and up-regulate MerTK in vitro.

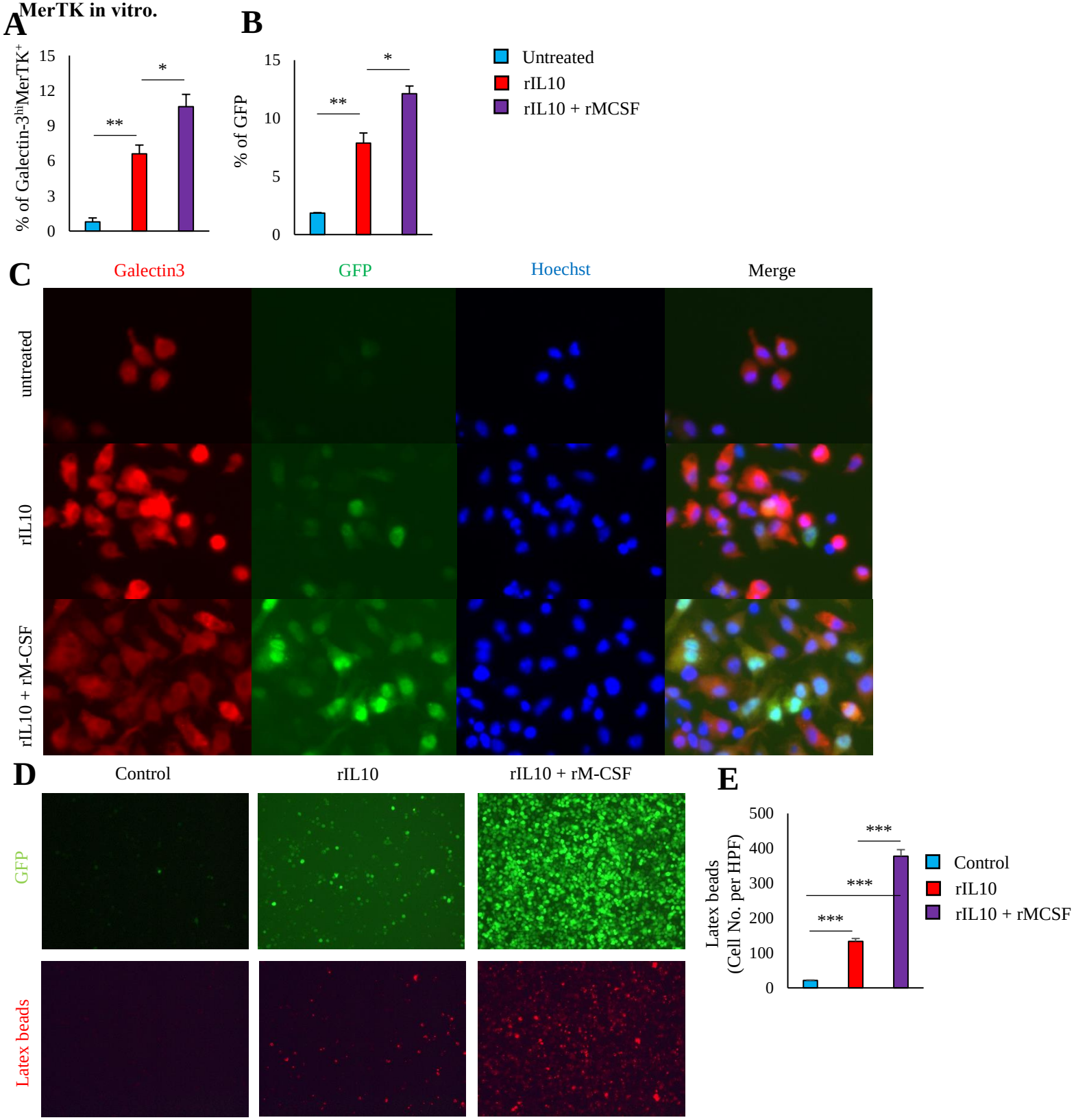

A, B CD11b$^+$Ly6G$^-$ cells (2 × 10^5) were sorted from bone marrow of 8- to 10-week-old EGFP-*Spp1*-KI reporter mice and cultured for 3 days with rIL-10 or rIL-10 + rM-CSF or left untreated. Bar graphs enumerate percentage of galectin-3^{hi} MerTK$^+$ cells (**A**) and *Spp1*-GFP (**B**) in CD11b$^+$Ly6G$^-$ cells by flow cytometric analysis (n = 5 per group). **C** CD11b$^+$Ly6G$^-$ cells (2 × 10^5) were sorted from bone marrow of 8- to 10-week-old EGFP-*Spp1*-KI reporter mice and cultured for 3 days with rIL-10 or rIL-10 + rM-CSF or left untreated. Analysis of a fluorescence microscopy demonstrated galectin-3, EGFP-*Spp1* expression, and Hoechst. **D** Latex beads were added in cultured CD11b$^+$Ly6G$^-$ cells sorted from bone marrow of 8- to 10-week-old EGFP-*Spp1*-KI reporter mice with indicated reagent for 4 hours. **E** Bar graphs enumerate the number of latex beads in high power field (n = 5 mice per group). *P < 0.05, **P < 0.01, ***P < 0.001; n.s.: not significant. Data are mean ± SEM.

Figure S5. Activation of STAT3 alone is insufficient for the induction of osteopontin in vitro.

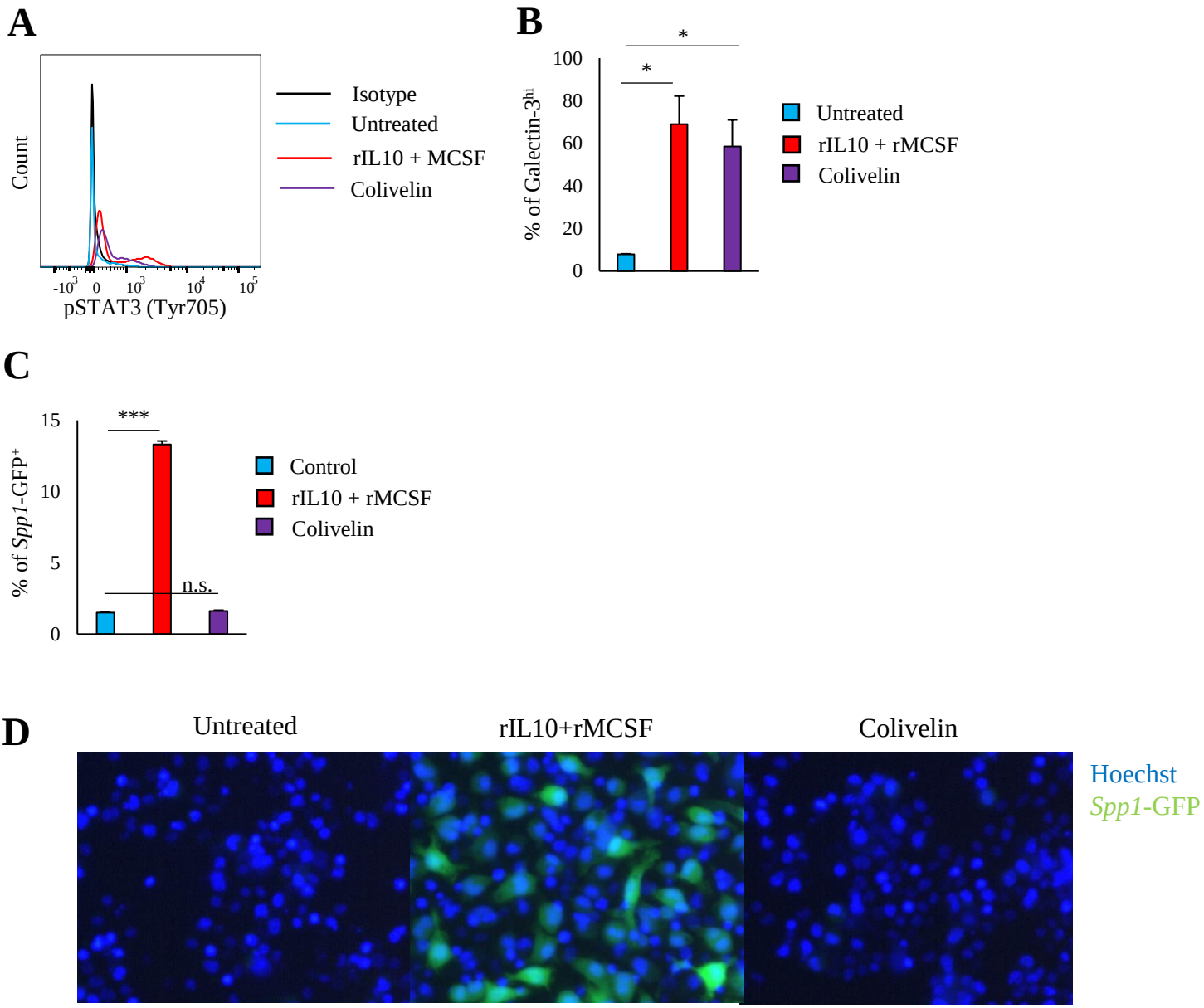

A-D 2 × 10^5 $CD11b^+Ly6G^-$ cells sorted from BM of EGFP-*Spp1*-KI reporter mice were cultured in IL-10 + M-CSF, Colivelin, or left untreated for 48 hours. **A** Representative histogram of pSTAT3 (Tyr705) in $CD11b^+Ly6G^-$ cells by flow cytometric analysis. **B, C** Flow cytometric analysis of galectin-3^{hi} (**B**) and *Spp1*-GFP expression (**C**) in $CD11b^+Ly6G^-$ cells. Bar graphs enumerate percentage of these cells (n = 5). **D** Analysis of a fluorescence microscopy demonstrated galectin-3, EGFP-*Spp1* expression, and Hoechst. *P < 0.05, ***P < 0.001; n.s.: not significant. Data are mean ± SEM.

Figure S6. ERK1/2 activation is required for Spp1 transcriptional activity in vitro.

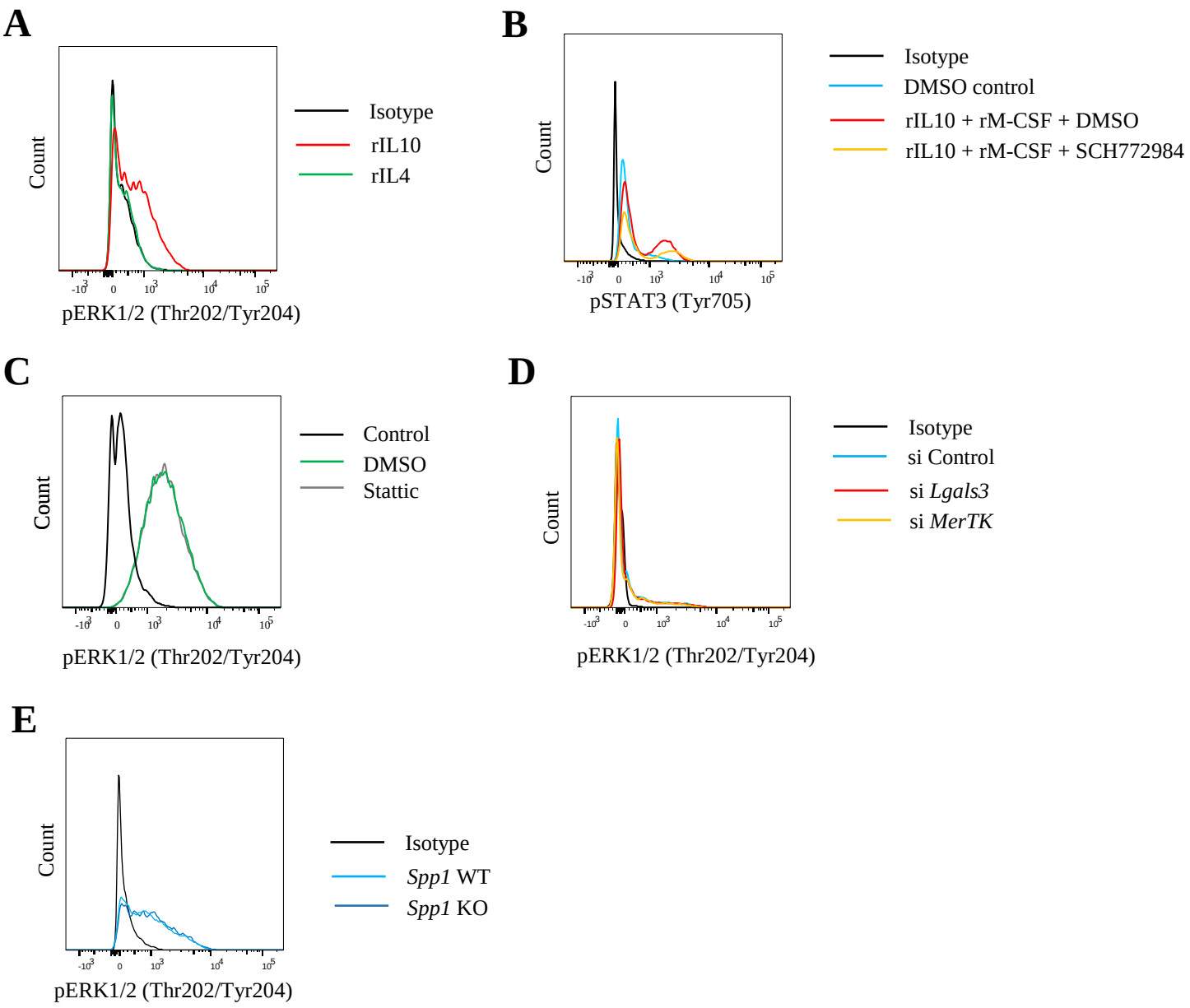

A $CD11b^{+}Ly6G^{-}$ cells (2×10^{5}) were sorted from bone marrow of 8- to 10-week-old WT mice and cultured for 3 days with rIL-4 or rIL-10. Representative histogram of pERK1/2 (Thr202/Tyr204) in $CD11b^{+}Ly6G^{-}$ cells by flow cytometric analysis. **B** $CD11b^{+}Ly6G^{-}$ cells (2×10^{5}) were sorted from bone marrow of 8- to 10-week-old WT mice and cultured for 3 days with rIL-10 + rM-CSF + DMSO, rIL-10 + rM-CSF + SCH772984 (ERK1/2 inhibitor) or DMSO. Representative histogram of pSTAT3 (Tyr705) in $CD11b^{+}Ly6G^{-}$ cells by flow cytometric analysis. **C** $CD11b^{+}Ly6G^{-}$ cells (2×10^{5}) were sorted from bone marrow of 8- to 10-week-old WT mice and cultured for 3 days with rIL-10 + rM-CSF + DMSO or rIL-10 + rM-CSF + Stattic (STAT3 inhibitor). Representative histogram of pSTAT3 (Tyr705) in $CD11b^{+}Ly6G^{-}$ cells by flow cytometric analysis. **D** $CD11b^{+}Ly6G^{-}$ cells (2×10^{5}) were sorted from bone marrow of 8- to 10-week-old WT mice and cultured for 3 days with rIL-10 + rM-CSF with siControl, si*Lgals-3*, or si*MerTK*. Representative histogram of pERK1/2 (Thr202/Tyr204) in $CD11b^{+}Ly6G^{-}$ cells by flow cytometric analysis. **E** $CD11b^{+}Ly6G^{-}$ cells (2×10^{5}) were sorted from bone marrow of 8- to 10-week-old WT or *Spp1* KO mice and cultured for 3 days with rIL-10 + rM-CSF. Representative histogram of pERK1/2 (Thr202/Tyr204) in $CD11b^{+}Ly6G^{-}$ cells by flow cytometric analysis. Flow cytometric analysis was performed in at least three independent experiments.

Figure S7. ERK1/2 activation is required for OPN transcriptional activity in vivo.

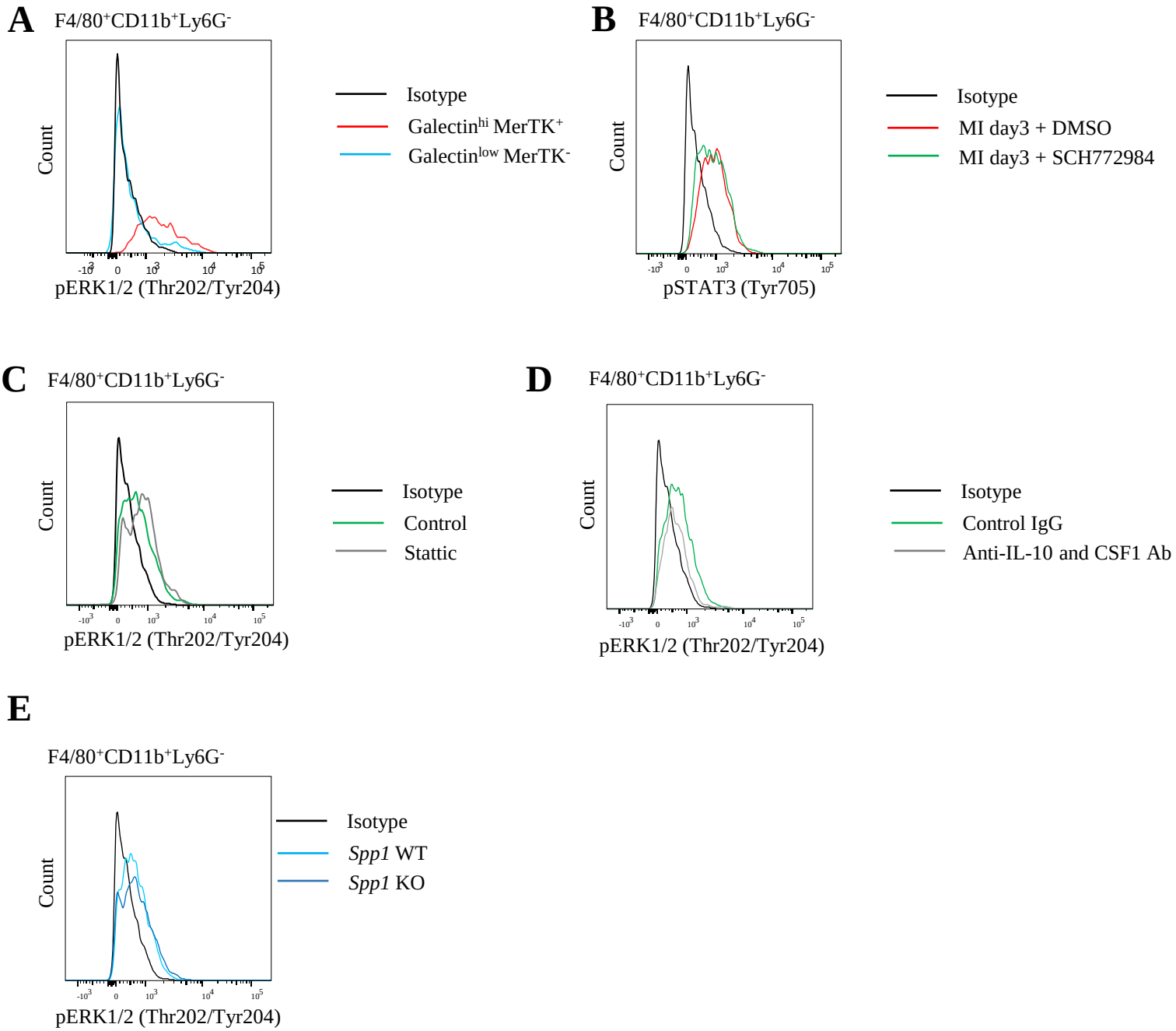

A Histogram of pERK1/2 (Thr202/Tyr204) on cardiac galectin-3^{hi}MerTK^{+} or galectin-3^{low}MerTK^{-} F4/80^{+}CD11b^{+}Ly6G^{-} cells of post-MI hearts on day 3. **B** DMSO or SCH772984 (ERK1/2 inhibitor) was administered via intraperitoneal injection from 1 day before MI to post-MI day 3 into EGFP-*Spp1*-KI reporter mice. Histogram of pSTAT3 (Tyr705) on cardiac F4/80^{+}CD11b^{+}Ly6G^{-} cells of DMSO or SCH772984-injected hearts. **C** DMSO or Stattic (STAT3 inhibitor) was administered via intraperitoneal injection from 1 day before MI to post-MI day 3 into WT mice. Representative histogram of pERK1/2 (Thr202/Tyr204) on cardiac F4/80^{+}CD11b^{+}Ly6G^{-} cells of DMSO or Stattic-treated mice. **D** Control IgG or anti-IL10 antibody or anti-IL10 and anti-M-CSF antibody was administered via intraperitoneal injection from 1 day before MI to post-MI day 3 into EGFP-*Spp1*-KI reporter mice. Histogram of pERK1/2 (Thr202/Tyr204) on cardiac F4/80^{+}CD11b^{+}Ly6G^{-} cells of control IgG or anti-IL10 antibody or anti-IL10 and anti-M-CSF antibody-injected hearts. **E** Histogram of pERK1/2 (Thr202/Tyr204) on cardiac F4/80^{+}CD11b^{+}Ly6G^{-} cells of post-MI hearts of *Spp1* WT or *Spp1* KO mice on day 3. Flow cytometric analysis was performed in at least three independent experiments.

Figure S8. rM-CSF treatment accelerates infarct repair after MI.

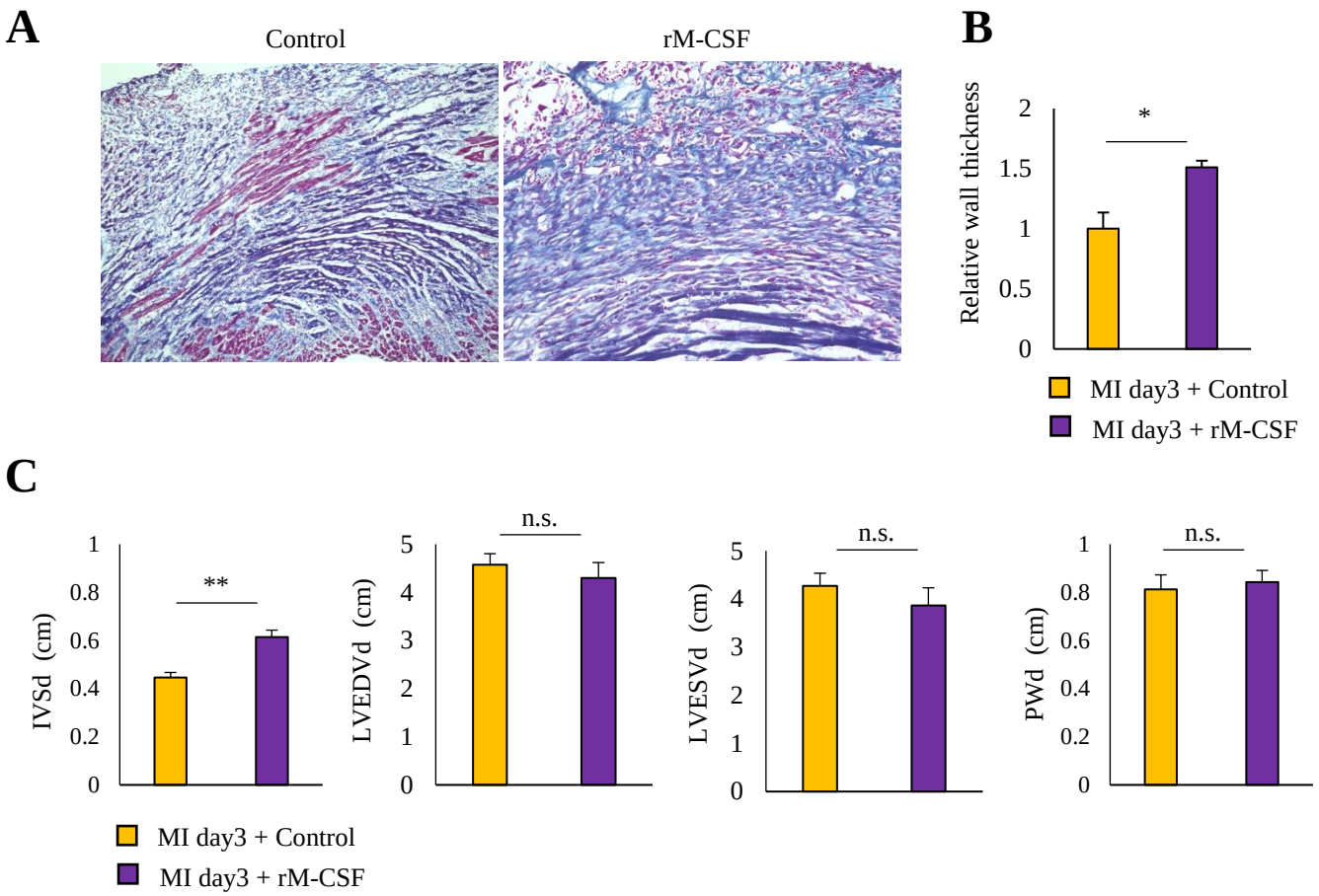

A Azan staining of post-MI heart on day 3 of EGFP-*Spp1*-KI reporter mice treated with control regent or rM-CSF. **B** Relative wall thickness of post-MI heart on day 3 of EGFP-*Spp1*-KI reporter mice treated with control regent or rM-CSF (*n*= 3 mice per group). **C** Echocardiographic data after MI on day 7 (*n*= 6 mice per group). LVESV, left ventricular end systolic diameter; LVEDV, left ventricular end diastolic diameter; IVSd, interventricular septum diameter; PWd, posterior wall diameter. **P* < 0.05, ***P* < 0.01; n.s.: not significant. Data are mean ± SEM.